

Light power behaviour when bending plastic optical fibres

J. Arrue
J. Zubia
G. Fuster
D. Kalymnios

Indexing terms: Light power, Plastic optical fibre, Bend loss

Abstract: The redistribution of light power and the radiated power along a bent section of a plastic optical fibre (POF) is analysed. In this context, a theoretical approach for understanding, and hence optimising, the major factors that affect the behaviour of sensors utilising losses in fibre bends is reported. With a brief comment on the bend loss model used, an implementation of a three-dimensional analysis for bend losses is presented, and the theoretical analysis is compared with experimental results. The spatial redistribution of the optical power in the bend is also calculated

1 Introduction

Compared with glass fibres, the large core diameter of plastic optical fibres (POF) makes them an easy to handle transmission medium, facilitates splicing together two or more fibre lengths, and allows the use of less accurate connectors. In addition, POFs are not only usually cheaper to produce than glass fibres, but they are also especially well suited for use with inexpensive LEDs, emitting in the visible region of the spectrum. Although nowadays graded-index POFs are used for high-bandwidth telecommunications, step-index POFs are usually preferred for the design of transduction mechanisms, using optical fibres to sense physical parameters. In this context, we report on a theoretical approach for understanding, and hence optimising, the major factors that affect the behaviour of sensors utilising losses in fibre bends. We briefly comment on the bend loss model used, present an implementation of a 3D analysis for bend losses, and compare our theoretical analysis with experimental results.

2 Relation between bending losses and optical sensors

Radiation losses along a bent section of a step-index

© IEE, 1998

IEE Proceedings online no. 19982476

Paper first received 12th February 1998 and in revised form 6th August 1998

J. Arrue and J. Zubia are with the University of the Basque Country, Spain

G. Fuster and D. Kalymnios are with the University of North London, UK

plastic optical fibre are usually calculated by means of a geometric approach. Light is treated as individual rays that propagate in zigzag paths, taking into account the changes in ray directions and probable radiation losses that take place at the reflection points on the core surface [1, 2]. The results for bending losses based on this theoretical approach can be represented as a function of a certain physical parameter, e.g. bend radius, which enables the design of optical sensors based on this parameter. Such sensors, based on bending losses, have been reported in the literature for measuring parameters such as the refractive index of a liquid [3–6]. Typically, such optical refractometers were implemented by shaping the optical fibre into an ideal U-shape. When using this configuration, the semicircular bend is usually stripped of its cladding and immersed in the liquid to be measured. If a longer bent section is desired, the preferred shape for the fibre is a semicircle plus a certain number of full turns, with the straight sections parallel, in order to occupy a small physical space. As a first simplified approach, the physical impossibility of having all the turns with any bend radius in exactly the same plane will not be taken into account. We will also neglect possible additional radiation losses due to the appearance of leaky rays (e.g. tunnelling rays) along any straight fibre section following the bend. These leaky rays would be caused by the discontinuity in the bend radius when the bend finishes, and by the redistribution of light power along the bend. The fibres we consider are 1 mm step-index high NA (0.47) POFs. These are considered to be especially well suited for sensors based on radiation losses, because their large core diameters simplify physical implementation. In such sensors, by measuring the ratio of input to output light power, one can obtain the unknown influencing parameter by comparison with previously calculated or measured results. For that purpose, it is necessary to know the power ratios corresponding to a useful range of values for the parameter under test.

3 Bend loss calculation method

3.1 Geometric approach

For bent step-index optical fibres, light power can be considered to flow along the core within tubes of parallel rays of infinitesimal cross-section, which can undergo radiation at reflection points [1, 7]. In the following, the word 'ray' refers to these infinitesimal tubes of rays. The basic method for calculating the reflection

points in this paper is the same as that already proposed in the literature [8], but our analytical approach has the advantage of not requiring knowledge of specific mathematical formulae. The mathematical simplicity of our approach makes it easy to generalise the method to other fibre shapes, such as that of a spiral-shaped POF rolled up in an optical fibre reel. This simplicity lies in obtaining the ray paths by using concepts of relative motion, which constitutes another approach to the aforementioned basic method as illustrated in Fig. 1. This Figure shows a portion of a torus representing a bent section of a POF, as well as the straight path followed by a light ray until it reflects for the first time during its propagation along the bend. The successive imaginary circular cross-sections of the torus are intersected by the light ray, during its propagation, at different distances from the centre of the circle. Only at the reflection point does the light ray intersect the corresponding circular cross-section on its circumference, and this yields a method for calculating the reflection point. By superimposing all the circular cross-sections, in order to have all the successive intersection points in the same plane, the geometric locus of all these coplanar points becomes a hyperbola. This reduces the calculation of the reflection point to the intersection between a hyperbola and a circumference. The three-dimensional point can be easily obtained from the two-dimensional one by using symmetry properties. In Fig. 1, three circular cross-sections are shown, as well as three small spots representing the corresponding intersection points between the ray path and the circular cross-sections.

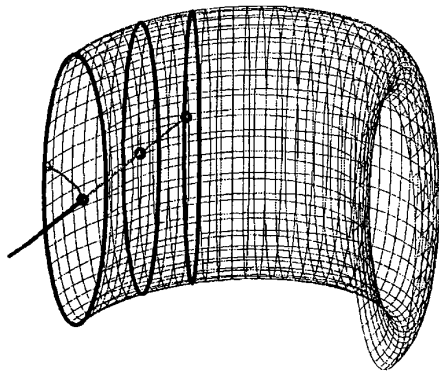


Fig. 1 Ray path calculation method 1

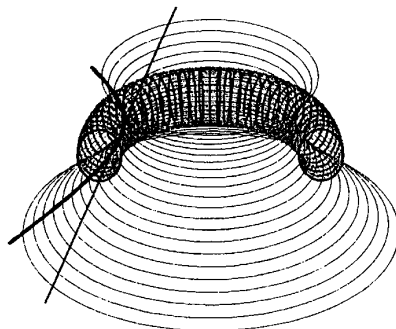


Fig. 2 Ray path calculation method 2

In our approach, the method for calculating this hyperbola is based on the fact that rotating the ray and not the plane leads to the same relative effect. In this

way, the necessity of considering all successive circular cross-sections generated by rotating the plane disappears, the hyperbola being obtained, instead, as the intersection between the hyperboloid generated by the rotating ray and any stationary plane containing a single circular cross-section, as shown in Fig. 2. The formulae to be used in the previously mentioned approach can be derived using our approach, but our method is easier to generalise to other fibre shapes. Our method serves for any number of turns, and for both meridional and skew rays, since meridional rays can be considered as rays with negligible skewness.

3.2 Application of the transmission coefficients

An important step in the analysis is the assignment of a certain input power to each ray entering the bend. This power, which depends on the angle θ with the fibre symmetry axis at the entrance of the bend, has been assumed to be proportional to $(\cos \theta)^\gamma$, with $\gamma = 1$, although we could have chosen any other value between 0 and 1, because the value of γ does not significantly affect our results. This distribution is believed to approximate the output of an LED [9]. Although there is a short length of fibre between the lambertian LED and the bend, which causes refracting rays to lose all their power before entering the bend, bound rays maintain their initial power along the straight section. In calculating the total radiation loss, we assume a high enough number of initially uniformly distributed rays, in principle more than 2 million rays. If we add the powers of all the rays entering and exiting the bend, then the total radiation loss is the ratio between these two sums. As we calculate the ratio of output to input power, arbitrary units of power can be used. Calculation of the fraction of power that each ray still conveys on exiting the bend is made by considering the following.

The loss of light power at each reflection of the ray considered depends on its angle α with the normal to the core surface. As is well known, rays will refract at the core surface if α is less than the critical angle α_c . In such a case, the fraction of power reflected back into the core is $P_r = P_i * (1 - T)$, where P_i is the power in the incident ray, and T is the power transmission coefficient. T is calculated from:

$$T = \frac{4 \cos \alpha (\cos^2 \alpha - \cos^2 \alpha_c)^{1/2}}{[\cos \alpha + (\cos^2 \alpha - \cos^2 \alpha_c)^{1/2}]^2} \quad (1)$$

assuming that the direction of the electric field is perpendicular to the plane of incidence [1]. For any other polarisation direction, the value of T would not differ significantly from that given by eqn. 1, especially when the refractive indices in the two media are similar, as proved in a previous paper [2].

If $\alpha > \alpha_c$, we can assume that $P_r = P_i$, since non-refractive rays will radiate a negligible amount of power, if any [1, 2, 10–12]. We can also neglect any absorption in the POF in relation to POF transparency, because the length of the bent section is very small. The total power reaching the exit of the bend is obtained by adding the powers remaining in each of the individual rays considered.

4 Theoretical and experimental results for bends of different radii and external refractive indices

4.1 Effect of the bend radius

When light is forced to propagate in a POF along a semicircular bend stripped of its cladding, the ratio of the output power to the input power (P_o/P_i) depends on the bend radius. This quotient is also a function of the refractive index of the outer medium, which could be a liquid in which the POF core is immersed, this fact being the basis of typical optical refractometers [3–6]. One of the goals in our analysis has been a better understanding of the effect of the bend radius on the output powers for a range of external refractive indices between 1.333 and 1.44. The lowest value is the refractive index of distilled water, and the highest value corresponds to a high concentration of a solute dissolved in water, such as a solution containing 85% of sugar.

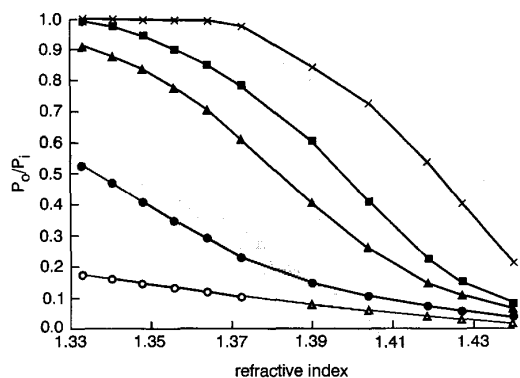


Fig. 3 Effect of the bend radius (0.5 turns)

A desirable characteristic of the ratio P_o/P_i corresponding to a given bend radius is its sensitivity to variations in the external refractive index, which is determined by the slope of the response of this quotient against the refractive index. Obviously, the steeper the curve the more accurately the refractive index can be calculated from experimental measurements. Fig. 3 shows the theoretically obtained quotients P_o/P_i corresponding to five different bend radii, using a semicircular bend. The core diameter is assumed to have a standard diameter of 1 mm, a value that corresponds to the usual core diameter of 980 μm , approximated here to 1 mm. This assumption does not imply loss of generality. Indeed we have established that the most important parameter in the loss calculations is the ratio of the bend radius to the core radius, and this can be used as a scaling factor to obtain the same fractional losses due to the bend. This fact can be utilised, for example, to experimentally simulate the losses due to a small bend radius by using a thicker POF, but with a greater bend radius.

The curves in Fig. 3 correspond, starting from the top, to bend radii of 15 mm, 9 mm, 7 mm, 4 mm and 1.75 mm, respectively, with a core size of 1 mm. It is interesting to observe that the larger bend radii give steeper slopes for the higher refractive indices, while, in contrast, the smaller bend radii yield more linear curves and no horizontal section over the low refractive indices. It could be said, therefore, that a very inaccurate sensor would result if we used the left side of the curve corresponding to 15 mm, but the right side

would have an adequate slope for the design of a precision refractometer. Similarly, although the curve for 1.75 mm does not provide a steep response over any part of the refractive index range, it does, however, yield a similar accuracy over the full refractive index range, and this may be advantageous in measuring the low refractive indices. Another observation from this Figure is that the curves in the low refractive index region change from convex to concave as the bend radius decreases. This fact suggests that a more linear response might be possible by using a bend radius between 7 and 4 mm, or even by adding a convex response curve to a concave one.

In Fig. 4, it is seen that the response for a bend radius of 4.25 mm is quite linear up to a refractive index of 1.39, but presents a gentle gradient over the highest refractive indices. Fig. 4 also shows a possible way to linearise the whole curve by adding the curves corresponding to 8 mm and 4.25 mm, resulting in another curve that is much more linear than the two separate ones.

Finally, in order to test the validity of our analysis, we have intentionally chosen a bend radius of 1.75 mm, in Fig. 3, since this value has been proposed and used in the literature for a refractive index sensor ranging from 1.3330 to 1.3723 [4]. This range coincides with the lowest part of our range of refractive indices. The experimental results that were presented were not absolute, but relative, and we have been able to compare these with our theoretical ones, and show very close agreement in the slope of the linear response.

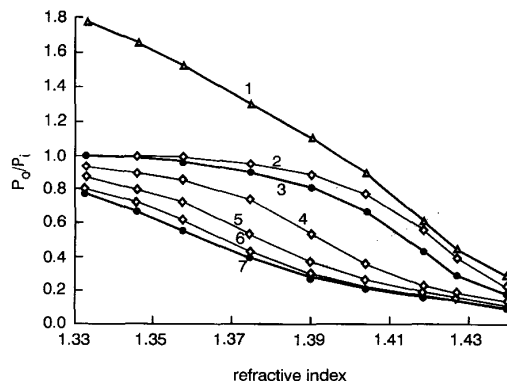


Fig. 4 Method to obtain a more linear curve by adding a concave one and a convex one
1) $R = 8 + R = 4.25$; 2) $R = 9$ mm; 3) $R = 8$ mm; 4) $R = 6$ mm; 5) $R = 5$ mm; 6) $R = 4.5$ mm; 7) $R = 4.25$ mm

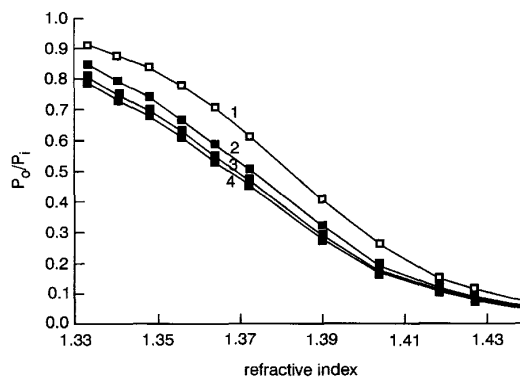


Fig. 5 Effect of the number of turns ($R = 7$ mm)
1) 0.5 turns; 2) 1.5 turns; 3) 2.5 turns; 4) 3.5 turns

4.2 Effect of the number of turns

Fig. 5 shows theoretical sets of ratios P_o/P_i corresponding to different numbers of turns in a typical step-index POF, stripped of its cladding, for the same range of refractive indices as before, and a bend radius of 7mm. From this Figure it is observed that, as the number of turns increases, the response is less affected by the addition of a new turn. This fact occurs because leaky rays contribute less and less to the total power as the distance increases, while bound rays remain bound all along the bend. Specifically, the uppermost curve, which corresponds to a semicircular bend (0.5 turns), differs from the curve just below more than this second curve does from the third one, although in both cases the difference in the number of turns is the same, namely 1 full turn. In the same way, the curves for 2.5 and 3.5 turns, the lowest ones in the Figure, are even closer to each other, thus indicating that the response curves tend to reach a stabilised state. This behaviour is interesting and suggests that the influence of an external parameter (bend radius, external refractive index, etc.) on the ratio P_o/P_i will only change significantly for changes in the number of turns between 0.5 and 2.5.

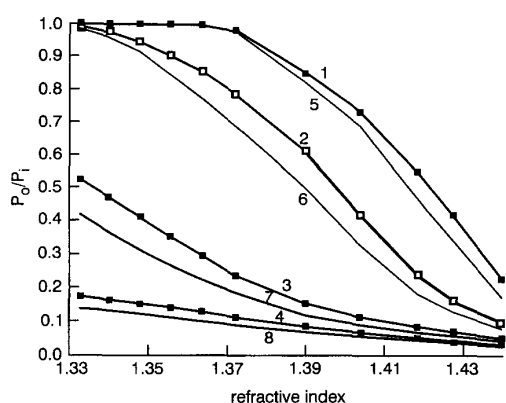


Fig. 6 Combined effect of the bend radius and the number of turns
 1) 0.5 turns; $R = 15\text{mm}$; 2) 0.5 turns; $R = 9\text{mm}$; 3) 0.5 turns; $R = 4\text{mm}$;
 4) 0.5 turns; $R = 1.75\text{mm}$; 5) 1.5 turns; $R = 15\text{mm}$; 6) 1.5 turns; $R = 9\text{mm}$;
 7) 1.5 turns; $R = 4\text{mm}$; 8) 1.5 turns; $R = 1.75\text{mm}$

4.3 Combined effect of the bend radius and the number of turns

In Fig. 6, we plot curves corresponding to four different bend radii, and two cases of different turns, namely 0.5 and 1.5, since adding more full turns would quickly lead to a stabilised state. It can be seen that the response curves are much less affected by increasing the number of turns than by changing the bend radius. It is interesting, however, to note that by increasing the number of turns one might obtain a slightly more linear response, as is the case for the bend radius of 9mm.

4.4 Checking the accuracy of the theoretical analysis

When one calculates bending losses by a ray tracing method, as in our case, it is necessary to allow a margin of error for not considering a high enough number of rays. The ideal number of rays should be approximately equal to the estimated number of modes N propagating along the fibre, which is given by $N \approx 0.5 * (\pi * d * NA / \lambda)$ [13]. For a wavelength of $\lambda = 650\text{nm}$, a numerical aperture $NA = 0.47$, and a fibre diameter $d = 1\text{mm}$, we obtain $N = 2.7 * 10^6$ modes. If the number of rays is so high, the computation process will be too

slow. Therefore, it is useful to know of the influence of the number of rays on the accuracy obtained. All calculations in this paper have been carried out with 10,000 uniformly-distributed skew rays, i.e., equally spaced both in the transverse plane and within the cone of power radiated from each transverse point. An estimation of the error introduced by limiting the number of rays to 10,000 has been obtained by comparing the corresponding results with those calculated for a much higher number of rays. Fig. 7 shows pairs of curves for 15mm, 9mm, 4mm and 1.75mm, respectively, starting from the top, and with the upper curve corresponding to 2.56 million rays and the one below it to 10,000 rays. It can easily be checked that with a bend radius greater than 9mm, 10,000 rays yield a result to within 10% of that for 2.56 million rays. We also note that the total computation time for 10,000 rays was 270 times less than that for 2.56 million rays.

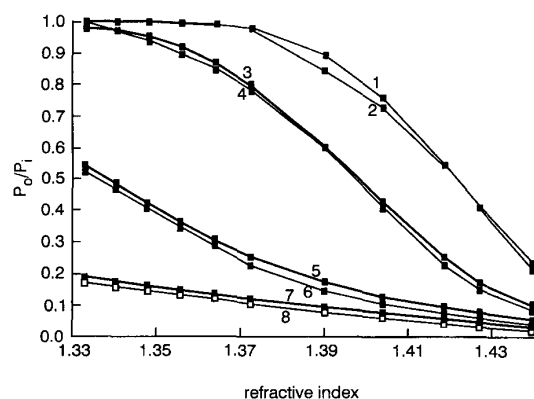


Fig. 7 Comparison between 10,000 rays (1°) and 2.56 million rays (2°)
 1) $R = 15\text{mm}$ (1°); 2) $R = 15\text{mm}$ (2°); 3) $R = 9\text{mm}$ (1°); 4) $R = 9\text{mm}$ (2°);
 5) $R = 4\text{mm}$ (1°); 6) $R = 4\text{mm}$ (2°); 7) $R = 1.75\text{mm}$ (1°); 8) $R = 1.75\text{mm}$ (2°)

The next step was to check the differences between the theoretical results and experimental measurements. For this purpose, we prepared fibre probes with several bend radii using the 1 mm step-index Mitsubishi Eska Extra POF ($n_{\text{core}} = 1.492$, $n_{\text{cladding}} = 1.417$), stripped of its jacket without damaging the cladding. We managed to create permanent semicircular bends by heat treatment for 1h at 75°C . However, we experienced serious practical difficulties in removing the cladding using solvents such as alcohol. In all cases tried, there was always uncertainty as to whether this layer was completely removed, and in many cases it was over-removed, and the core was damaged. In consequence, it was decided to keep the cladding on and modify the computer program slightly to take into account the presence of the cladding. Although new approaches have to be introduced into the calculation, an agreement between the new results and the experimental ones can serve as a partial verification of the computer simulation.

Given the above, we modified the analysis to take into consideration the core-cladding-liquid interfaces. First, rays refracted at the core-cladding interface, although they change their direction, reach the cladding-liquid interface and can be reflected back into the POF. Secondly, for any liquid refractive index higher than that of the cladding, no significant reflection occurs, and the loss curve should start to become horizontal if plotted against the liquid refractive index. Therefore, we included the second reflection in the

computer simulation, calculating the corresponding new incidence angle and obtaining the power lost by the ray at both interfaces. We also assumed, for simplicity, that rays arising from the second reflection were reflected in the same direction and from the same position as those arising from the first reflection. This approach, although very approximate, is used because the cladding is very thin in relation to the core ($20\mu\text{m}/980\mu\text{m}$). In addition, we found that we had to multiply all the calculated reflection coefficients by the same constant (0.59) in order for our theoretical curves to coincide with the experimental ones. An intuitive explanation for this factor arises from the observation of Fig. 8. When ray 1 is only slightly refracting, the refracted ray is nearly parallel to the interface and re-enters the fibre at a considerable distance from the refraction point. Therefore, when considering for simplicity that ray 3 starts from the same point as ray 2, we are assuming more reflections than in reality, so we need a factor less than unity to compensate for the excess of calculated losses. Both the experimental results with cladding and the theoretical ones including the correction factor are shown in Fig. 9.

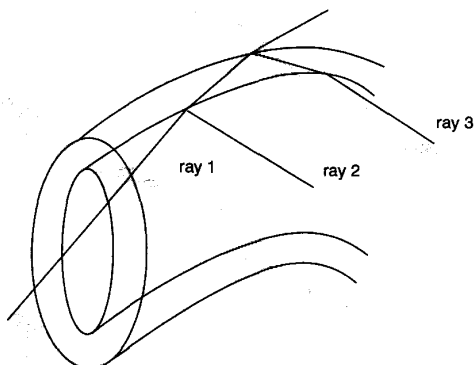


Fig. 8 Justification of the factor used to adjust theoretical and experimental results

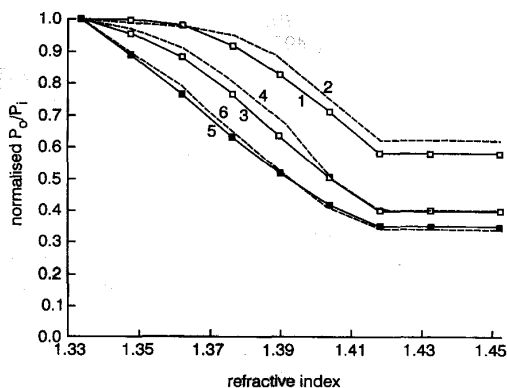


Fig. 9 Comparison between experimental and theoretical results
1) $R = 12\text{mm}$; 2) experimental; 3) $R = 7\text{mm}$; 4) experimental; 5) $R = 4\text{mm}$; 6) experimental

In Fig. 10, it is shown graphically how the power transmission coefficient at the reflection points, i.e. T , varies with angle of incidence and with outer refractive index. More specifically, we plot $1 - T^{40}$, which would correspond to 40 identical reflections in an uncladded POF, this number representing a possible number of reflections for a given ray in the semicircular bends that we will consider later. This Figure serves to confirm our theory in the sense that the more linear curves

are obtained for the more perpendicular rays to the interface, i.e., for sharp bends, whereas the greater slopes are obtained at the back part of the Figure, i.e., for greater bend radii.

5 Conclusions

We have generalised a recently published method for evaluating the characteristics of bent optical fibres, and have further developed it by incorporating some simplifications. As a result, our analysis greatly simplifies the mathematical complexity of the problem, and thus reduces computational time considerably. We have adopted our analysis for characterising the behaviour of liquid refractive index sensors utilising bent sections of fibre. Although the fibres used in our examples are plastic with large core diameter, the analysis is also applicable to other types of fibres. It has been shown that by understanding the propagation characteristics of light around bends, it is feasible to optimise the response of particular types of sensors that use high losses in fibre bends as the sensing mechanism. Specifically, we have shown that a reasonably linear curve, for a 1mm POF over a large range of external refractive indices, can be obtained by adding the responses for $R = 8\text{mm}$ and $R = 4.25\text{mm}$, which can be easily implemented in practice. We have also shown that increasing the number of turns over 2.5 has very little effect on the response.

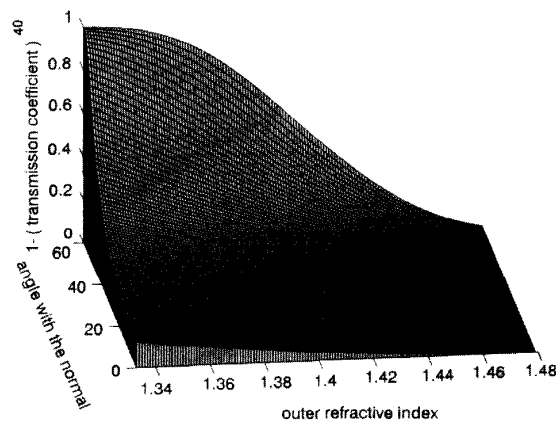


Fig. 10 Estimation of the power remaining after 40 reflections as a function of outer refractive index and angle with the normal, in the case that all reflections are identical

Experimental results obtained with bends of various radii and various refractive indices surrounding the bend core have provided convincing evidence for the validity of our analysis.

6 Acknowledgments

J. Zubia and J. Arrue wish to thank the financial support for this work given by Gobierno Vasco and by Universidad del País Vasco, under projects UE96/38 and UPV 147.345-EA 104/97 ZUBIA, respectively.

7 References

- 1 SNYDER, A.W., and LOVE, J.D.: 'Optical waveguide theory' (Chapman and Hall, London, 1983, 2nd edn.)
- 2 ARRUE, J., and ZUBIA, J.: 'Analysis of the decrease in attenuation achieved by properly bending plastic optical fibres', *IEE Proc., Optoelectron.*, 1996, **143**, pp. 135-138

- 3 TAKEO, T., and HATTORI, H.: 'Silica glass fiber photorefractometer', *Appl. Opt.*, 1992, **31**, (1), pp. 44-50
- 4 BAYLE, J.J., and MATEO, J.: 'Plastic optical fibre sensor of refractive index, based on evanescent field'. 5th international conference on *Plastic optical fibers*, Paris, France, 1996, pp. 220-227
- 5 HARMER, A.L.: 'Optical fibre refractometer using attenuation of cladding modes'. Battelle Research Institute, Geneva, Switzerland
- 6 GUPTA, B.D., and SINGH, C.D.: 'Fiber-optic evanescent field absorption sensor: a theoretical evaluation', *Fiber Integr. Opt.*, 1994, **13**, pp. 433-443
- 7 GHATAK, A., SHARMA, E., and KOMPPELLA, J.: 'Exact ray paths in bent waveguides', *Appl. Opt.*, 1988, **27**, (15), pp. 3180-3184
- 8 MARCOU, J., and MICHELET, K.: 'A new method to evaluate the bends in polymer optical fibers'. 5th international conference on *Plastic optical fibers*, Paris, France, 1996, pp. 205-212
- 9 NAKAMURA, A.: 'Power coupling between an LED and a plastic optical fibre'. 3rd international conference on *Plastic optical fibers*, Yokohama, Japan, 1994, pp. 115-117
- 10 SNYDER, A.W., and LOVE, J.D.: 'Tunnelling leaky modes on optical waveguides', *Opt. Commun.*, 1974, **12**, (3), pp. 326-328
- 11 BOECHAT, A.A.P., SU, D., HALL, D.R., and JONES, J.D.C.: 'Bend loss in large core multimode optical fiber delivery systems', *Appl. Opt.*, 1991, **30**, pp. 321-327
- 12 GLOGE, D.: 'Bending loss in multimode fibers with graded and ungraded core index', *Appl. Opt.*, 1972, **11**, (11), pp. 2506-2513
- 13 GLOGE, D.: 'Optical power flow in multimode fibers', *Bell Syst. Tech., J.*, 1972, **51**, pp. 1767-1783